



Use of bi-Seasonal Landsat-8 Imagery for Mapping Marshland Plant Community Combinations at the Regional Scale

Sébastien Rapinel^{1,2} · Jan-Bernard Bouzillé¹ · Johan Oszwald² · Anne Bonis¹

Received: 9 March 2015 / Accepted: 31 August 2015 / Published online: 8 September 2015
© Society of Wetland Scientists 2015

Abstract Coastal marshlands may provide ecosystem services but their vegetation and related services may be impacted by environmental changes. Habitat mapping is a key step to monitor the spatio-temporal dynamics of vegetation and detect on-going changes. However, it is still a challenge to produce reliable vegetation maps at the regional scale. This study aims to evaluate the potential of new Landsat-8 imageries (acquired in September and December 2013) for mapping fine-grained plant communities in coastal marshlands. Field-based vegetation maps were collected for 270 km of marshlands along the French Atlantic coast. In order to be identifiable on the satellite image, fine-grained vegetation units were aggregated into fewer plant community combinations. The classification accuracy was assessed by comparison with field-based vegetation data and compared between the supervised methods used, including Minimum Distance, Mahalanobis, Maximum Likelihood, Random Forest and Support Vector Machine. The best result was obtained with the Maximum Likelihood classifier and by combining the two Landsat-8 images (85.9 % accuracy overall). Three main habitat types dominated the coastal Atlantic marshlands: croplands, *Trifolium maritima*e-*Oenantheto silaifoliae* geosigmetum and *Puccinellio maritima*e-*Arthrocnemeto fruticosi* geosigmetum. The reliability of the vegetation map produced will provide a good basis for monitoring the conservation status of the various habitats.

Keywords Coastal marshlands · Conservation · Geosigmetum · Habitat directive 92/43/EEC · Phytosociology

Introduction

Coastal marshlands provide patrimonial, ecological and ecosystem services (Mitsch and Gosselink, 2007), and are thereafter part of the European Natura 2000 framework (http://ec.europa.eu/environment/nature/natura2000/index_en.htm) but also in the context of global mapping of saltmarshes (<http://data.unep-wcmc.org/>). Coastal marshlands are vulnerable habitats with regards to anthropogenic pressures (Lee and Yeh, 2009), natural hazards (Chauveau et al., 2011) and rising sea levels (Kirwan et al., 2010). The mapping of coastal habitats appears thus essential for risk assessments as maps can be used to monitor the vegetation structure and to evaluate management impacts. Maps established from field surveys generally concern areas of limited extent, i.e. several hectares, and accordingly, they focused on the most endangered marshes. However, monitoring requirements concerns marshlands as a whole and there is a clear need for coastal vegetation maps that take fine vegetation patterns into account while covering larger areas.

No method is currently available to produce such reliable and detailed vegetation maps at the regional scale for fine-grained vegetation, as in coastal areas in France. At the national level, a vegetation map was produced more than 25 years ago at the 1:500,000 scale (Ozenda and Lucas, 1987) and was recently integrated into the Geographical Information System (Leguédou et al., 2011). However, in this broad-scale map, coastal marshlands are mapped as a homogeneous vegetation type while some field studies (e.g. Bouzillé et al., 2001; Sawtschuk and Bioret, 2012) have shown that a diversity of coastal vegetation types must be distinguished.

✉ Sébastien Rapinel
sebastienrapinel@gmail.com

¹ UMR 6553 CNRS ECOBIO, Université Rennes 1, avenue du général Leclerc, 35000 Rennes, France

² UMR 6554 CNRS LETG, Université Rennes 2, place du recteur Henri Le Moal, 35000 Rennes, France

Remote sensing appears to be a promising opportunity for producing detailed and reliable vegetation maps over a larger area (Xie et al., 2008), specifically within the framework of the Natura 2000 habitat monitoring (Vanden Borre et al., 2011). Accordingly, plant communities have been successfully mapped in saltmarshes using hyperspectral images (Roelofsen et al., 2014). Increases in the seagrass distribution were observed from a SPOT-5 time series (Barillé et al., 2010), and vegetation formations were mapped in dunes and brackish marshes using Worldview-2 images (Rapinel et al., 2014). Such detailed vegetation maps were produced using very high spatial resolution images with a spatial extent limited to 20×20 km; they are therefore not suitable for producing affordable repeated mapping at a regional scale. Conversely, Landsat images are available for free and are suitable for characterizing broad-grained plant community patches at the regional scale (Zak and Cabido, 2002; Isacch et al., 2006; Berberoglu et al., 2004).

The major limitation of Landsat images is their spatial resolution which is generally considered too coarse for mapping heterogeneous habitats: this objective is therefore still a challenge (Lang et al., 2015) and was addressed in this work. The procedure that we tested in this work consisted in aggregating fine-grained vegetation units that constitute repetitive combinations at a higher hierarchical level. In most Landsat-based studies, the vegetation is aggregated according to physiognomy: Baker et al. (2006) mapped woods, herbaceous and crops; Ottinger et al. (2013) discriminated saline meadows from shrubs and broadleaved trees; Cardoso et al. (2013) classified mangroves, marshes and dunes; Akumu et al. (2010) characterized dunal wetlands, forested wetlands and coastal swamp; Sanchez-Hernandez et al. (2007) identified saltmarshes and fens. Aggregation criteria may also be based on structural types, i.e. repetitive combinations of growth forms and other topographic attributes (Cingolani et al., 2004). However, neither structural or physiognomy-based typologies are suitable for ecological monitoring as no information is provided regarding plant community composition which therefore precludes any interpretation regarding the conservation status and composition-related services. At the opposite, in the Braun-Blanquet approach a typology of landscape units has been developed based on the occurrence of associations and other syntaxa and distinguishing characteristic syntaxon combinations, so-called sigmetum. Such vegetation complexes are united into geosigmetum, being the phytosociological characterization of larger landscape types (Van der Maarel, 2005; Géhu, 2011). In coastal marshlands, the plant community combinations (geosigmetum) are larger than the Landsat pixel size and (i) can be discerned from coarse resolution remote sensing data, such as a Landsat-8 image (Fig. 1), and (ii) can be associated with synthetic tables providing the composition of each plant community.

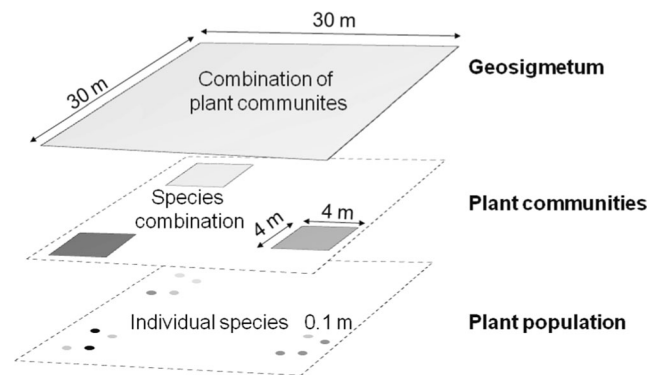


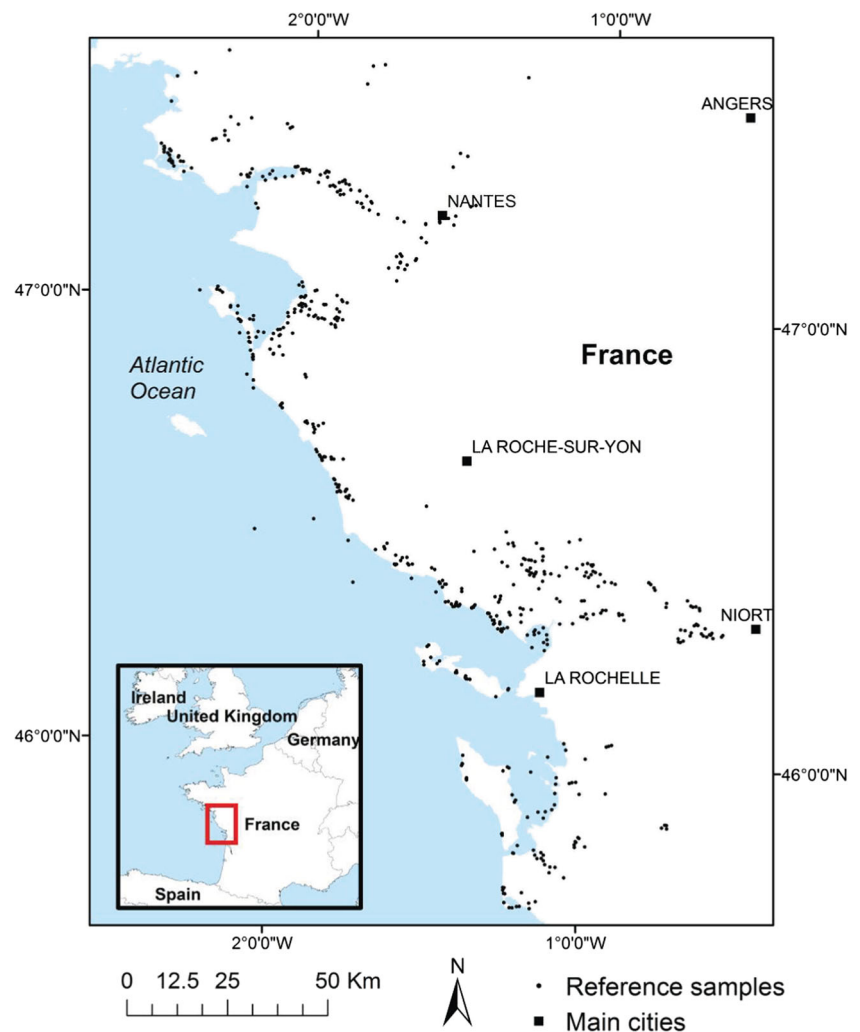
Fig. 1 Multi-scalar combinations of vegetation in relation to the spatial resolution of the remote sensing images

This geosymphytosociological method has already been used for mapping riparian forests using a field approach (Decocq, 2002), monitoring renaturalization processes in abandoned fields (Biondi et al., 2011), and monitoring herbaceous plant community patterns in coastal marshlands (Géhu et al., 1991). Surprisingly, it has rarely been combined with a GIS-based approach (but see Schmidlein, 2003). In particular, no attempts have yet been made to map combinations of plant communities from remote sensing while the spatial extent of a geosigmetum may show a good fit with the Landsat pixel size. We will use the Landsat-8 OLI satellite data, available since February 2013, which provides images with a spatial resolution of 30 m and a high spectral depth: here, we investigated the ability of two images Landsat-8 OLI acquired at two different seasons to map fine-grained and heterogeneous vegetation, aggregated into combinations of plant communities.

Study Site

The study area corresponds to a large part of the Atlantic coastal marshes in France, stretching from 47.4 to 45.6°N (Fig. 2). Four major NATURA 2000 sites are included in the studied area: Brière marsh, Breton Vendéen marsh, Poitevin marsh, and Brouage marsh, due to their interest with regards to waterbirds and natural and semi-natural habitats (Duncan et al., 1999). The climate is oceanic temperate, with a mean monthly minimum/maximum temperature ranging from 2/10 °C in winter to 12/24 °C in summer. The annual mean precipitation ranges from 700 to 900 mm with a summer water deficit. The coast is dominated by meso- macro-tides ranging from 2.8 to 6.6 m NGF (NGF: ‘Nivellement Général de la France’, which is the elevation above the Mediterranean mean sea level). The soil is clay-rich with locally, some peat soil (Verger, 2005). Several centuries ago, these coastal marshes were covered by mud flats and salt marshes. Then, following the construction of successive embankments, marshlands became occupied by natural grasslands, sown grasslands and

Fig. 2 Study site location and reference samples used for the Landsat classifications



crops (Godet and Thomas, 2013). Grasslands are nowadays managed as pastures or mown. The vegetation in these marshlands is composed of forested and perennial-dominated herbaceous species driven by the soil salinity, flooding pattern (Amiaud et al., 1998, Bouzillé et al. 2001) and grazing pattern (Marion et al. 2010, Dumont et al., 2012). These marshlands are locally drained and the winter flooding duration varies across locations.

Methodology

Linking Vegetation Typology with Landsat-8 Resolution

Marshland vegetation was described from the field relevés. Thereafter, plant community combinations of Atlantic coastal marshes were previously identified according to Géhu et al. (1991) based on phytosociological surveys and the associated analytical tables provided (Table 1). Four plant community combinations were identified, spread along a salinity gradient

and named according phytosociological nomenclature defined by Rivas-Martinez (2005): (i) close to the sea shore, plant community combinations characterizing the *Beto maritimae-Agropyretum pungentis* geosigmetum include halophilic communities such as *Spartinetum maritimae*, *Puccinellio-Arthrocnemetum perennis*, *Bostrichio-Halimionietum portulacoidis*, *Beto-Agropyretum pungentis* and occasionally including sub-halophilic communities; (ii) *Puccinellio maritimae-Arthrocnemeto fruticosi* geosigmetum typical of brackish habitats are mainly characterized by the following associations: *Juncetum gerardii*, *Parapholiso-Hordeetum marini*, *Festuca littoralis*, *Agropyro-Suaedetum verae*, *Puccinellio-Arthrocnemetum fruticosi*, *Salicornietum ramosissimae*, *Halimione-Puccinellietum maritimae*, without the plant communities typical of salt habitats; (iii) *Trifolio maritimae-Oenantheto silaifoliae* geosigmetum typical of sub-brackish habitats, in which halophilic associations become scarce and give way to *Alopecuro-Juncetum gerardii*, *Trifolio-Oenanthetum silaifoliae*, *Ranunculo-Oenanthetum fistulosae*, *Carici-Lolietum perennis* associations; (iv)

Table 1 Synoptic table highlighting the combinations of vegetal associations for the French Atlantic marshes (expressed as the percentage occurrence of plant communities: I - 1 to 20 %; II - 21 to 40 %; III - 41 to 60 %; IV - 61 to 80 %; V - 81 to 100 %), adapted from Géhu et al. (1991). The correspondence between each plant community and the CORINE Biotope and EUNIS codes are indicated

Habitat types		<i>Beto maritimae-Agropyreto pungentis</i> geosigmetum	<i>Puccinellio maritimae-Arthrocnemeto fruticosi</i> geosigmetum	<i>Trifolio maritimae-Oenantheto silaifoliae</i> geosigmetum	<i>Senecio aquatici-Oenantheto silaifoliae</i> geosigmetum	
Sites		BV BR	N BV	BV BR P	BV P	
CORINE	EUNIS	Plant communities				
Halophilic associations						
15.21	A2.6543	<i>Spartinetum maritimae</i>				III
15.622	A2.627	<i>Puccinellio-Arthrocnemum perennis</i>				III
15.621	A2.627	<i>Bostrychio-Halimionietum portulacoidis</i>				II
15.35	A2.611	<i>Beto-Agropyretum pungentis</i>				IV IV
15.321	A2.645	<i>Halimione-Puccinellietum maritimae</i>				V IV V III
15.1112	A2.6513	<i>Salicornietum ramosissimae</i>				IV V V
15.624	A2.627	<i>Puccinellio-Arthrocnemum fruticosi</i>				I IV I
15.623	A2.614	<i>Agropyro-Suaedetum verae</i>				V V V III
15.333	A2.63A	<i>Festucetum littoralis</i>				I III IV IV
15.331	A2.63B	<i>Juncetum gerardii</i>				II III V II
15.13	A2.653	<i>Parapholis-Hordeetum marini</i>				III III V V II I V
Meadow associations						
15.52	A2.623	<i>Alopecuro-Juncetum gerardii</i>				II V III III V
15.52	A2.623	<i>Trifolio-Oenanthetum silaifoliae</i>				I V V III V
15.52	A2.623	<i>Ranunculo-Oenanthetum fistulosae</i>				III V III V
15.52	A2.623	<i>Carici-Lolietum perennis</i>				V I V
37.21	E3.41	<i>Senecio-Oenanthetum silaifoliae</i>				IV IV
37.21	E3.41	<i>Gratiolo-Oenanthetum fistulosae</i>				III IV
37.21	E3.41	<i>Hordeo-Lolietum perennis</i>				I IV
37.21	E3.41	<i>Eleocharo-Oenanthetum fistulosae</i>				IV
Subaquatic associations						
53.17	B1.84	<i>Scirpetum maritimi compacti</i>				II V V III V
53.11	A4.551	<i>Phragmitetum australis</i>				I IV V IV II II
53.13	C3.23	<i>Typhaetum angustifoliae</i>				I V II V II
53.145	C3.24	<i>Butometum umbellati</i>				I I V I III
53.11	A4.551	<i>Scirpetum lacustris</i>				III III III II II
53.219	D5.21	<i>Althaea officinalis</i> and <i>Carex otrubae</i> community				V III V III V
53.213	D5.21	<i>Caricetum ripariae</i>				II III III IV
53.16	C3.26	<i>Phalaridetum arundinaceae</i>				III III IV
53.15	C3.25	<i>Glycerietum maximae</i>				I V
37.1	E5.421	<i>Symphytum officinale</i> community				IV
Aquatic associations						
23.211	A4.54	<i>Chaetomorpha-Rupprietum</i>				V V
22.432	A4.553	<i>Callitricho-Ranunculetum baudotii</i>				IV V I
24.44	C2.34	<i>Callitrichetum obtusangulae</i>				I I II III V
24.44	C2.34	<i>Lemnetum gibbae</i>				III III II I V
22.41	C1.22	<i>Lemnetum trisulcae</i>				I V II I V I

BV Breton-Vendéen marsh, BR Brouage marsh, N Noirmoutier marsh, P Poitevin marsh

Senecio aquatici-Oenantheto silaifoliae geosigmetum typical of fresh habitats, with alkaline Atlantic vegetation characterized by the combination of two associations: *Senecio-Oenanthetum silaifoliae* and *Gratiolo-Oenanthetum fistulosae*.

In order to include all of the possibly occurring vegetation types, nine other broader habitat classes were distinguished based on their physiognomy: “water bodies” with both salt and fresh water bodies; “Salt pans”; “Reeds” dominated by *Phragmites australis*, *Glyceria maxima* and *Typhetum latifoliae*, “Evergreen woods” including forest dominated by *Pinus maritima* and *Quercus ilex*, “Deciduous woods” including *Salix alba*, *Alnus glutinosa* and *Populus alba*-dominated stands; “Vegetal dunes” including *Ammophila arenaria* and *Helichryson staechadis*-dominated stands; “Crops”; “Sands”; and “Impervious” which includes urbanized areas and roads.

Vegetation Reference Data

Recent field-based vegetation maps were used to calibrate and validate the classifications of the Landsat images. Such fields base maps were produced after phytosociological field surveys performed between 2001 and 2012 in various Natura 2000 sites. They were delivered at the 1:25,000 scale using either the EUNIS or CORINE biotope referentials. Since vegetation may have changed from the production time, vegetation maps delivered prior 2009 were updated using very high spatial resolution images and additional phytosociological relevés (Table 2). Very high spatial resolution satellite images (<1 m) available from Google Earth were used for visual interpretation of the physiognomy-based habitat classes. In

addition, phytosociological relevés were carried out between May 2011 and June 2015 on grassland habitat types according to the Braun-Blanquet method by selecting quadrats of 4 × 4 m within each type of habitat. These additional relevés were performed in late spring, at the peak standing crop and when plant species identification is the easiest. As no phytosociological relevés were available since 2002 on the Rochefort marsh reference map, this reference data was used only for non-grassland habitats.

Remote Sensing Analysis

The satellite imagery was recorded by the Operational Land Imager (OLI) sensor on board the Landsat-8 with a 30 m spatial resolution. We selected two cloud-free images acquired on September 3 and December 8, 2013. These two images were delivered by the United States Geological Survey (USGS) and orthorectified to the UTM-30 N coordinate system (Level 1 T). Radiometric and atmospheric calibrations were performed on both Landsat images based on the MODTRAN radiative transfer model and the Landsat 8 spectral filter functions. The parameters were specified for: the mid-latitude summer and mid-latitude winter atmospheric model for September and December images respectively; and the rural aerosol model. For each date, the Landsat-8 strip included two adjacent scenes (200 × 400 km each) that covered the whole study area. Compared to the Landsat TM and ETM sensors, the new OLI sensor records images with a deeper spectral depth (12 bits). The September 3 Landsat 8 image was acquired at a low tidal level (3.0 m), when all saltmarshes were visible. The image acquired on December

Table 2 Date of field based vegetation map and additional field relevés and satellite images

Natura 2000 site	Area (km ²)	Year of production of field-based vegetation map	Date of update by additional phytosociological relevés	Date of update by analysis of VHSR satellite images
Loire estuary	217	2001	05/2011 (<i>n</i> = 55)	25/05/2011 (Worldview-02) 25/04/2013 (Worldview-02)
Breton Vendéen marsh and Noirmoutier	523	2009		25/05/2011 (Worldview-02) 02/07/2011 (Worldview-02) 03/06/2013 (Geoeye-01)
Sauzaie-Jaunay marsh	12	2010	07/2012 (<i>n</i> = 34)	03/06/2013 (Geoeye-01)
Poitevin marsh	780	2003	06/2013 (<i>n</i> = 113) 06/2014 (<i>n</i> = 348) 06/2015 (<i>n</i> = 49)	16/05/2014 (Rapideye)
Rochefort marsh	136	2002		13/10/2010 (Geoeye-01) 05/07/2011 (Worldview-02)
Charente marsh	107	2010		14/09/2011 (Worldview-02) 05/07/2011 (Worldview-02)
Brouage marsh and Oléron	260	2012		14/09/2011 (Worldview-02) 05/07/2011 (Worldview-02)
Seudre marsh	139	2010		14/09/2011 (Worldview-02) 05/07/2011 (Worldview-02)
Arvert	97	2009		14/09/2011 (Worldview-02)

8 corresponds to a high tide period (4.5 m NGF), when the lower saltmarshes were submerged.

In addition, a Digital Terrain Model (DTM) derived from the Shuttle Radar Topography Mission (SRTM) was used to delineate the marshlands because it has the advantage of being freely available worldwide. This DTM shows a 90 m horizontal resolution. It was produced from the Consultative Group on International Agricultural Research (Jarvis et al., 2008).

In a first step, coastal marshlands were delimited from the combination of both land and tidal marsh layers based on topographic and coastline distance criteria respectively. For this purpose, all DTM values above 6 m have been masked according to reference data and field expert knowledge. Indeed, coastal marshes are characterized by strong internal diversity and heterogeneity of habitats, while their geomorphological components are wide (> 3 km) and homogeneous. Moreover, their outer boundary with non-wetlands are well marked by hillsides with a significant elevation differences ($\Delta > 10$ m). In this geomorphological context, the use of SRTM data with a 90 m spatial resolution seems suitable for the delineation of coastal marshes at regional scale. Since the intertidal area width ranges from 100 to more than 2500 m, a 3000 m buffer area from the coastline, defined from the highest foreshore and available from the IGN, was added to integrate tidal saltmarshes.

In a second step, marshlands were characterized from the classification of Landsat 8 images. All seven multispectral bands, ranging from coastal blue to middle infrared spectra were included in the classification process. In order to investigate the ability of bi-seasonal Landsat images for the mapping of plant communities' combinations, September and December images were placed in a single dataset resulting from 14 band composite imagery. We then compared five of the most frequently used supervised classifiers: Minimum Distance (MID), Maximum Likelihood (ML), Mahalanobis Distance (MAD) (Richards 1999), Random Forest (RF) (Breiman, 2001) and Support Vector Machine (SVM) (Mountrakis et al., 2011). Samples were defined as 30×30 m areas from field-based vegetation maps in accordance with the Landsat OLI pixel size. To avoid edge effects and mixed pixels, all samples ($n = 559$) were selected within a 3×3 homogeneous pixel window size on both Landsat images. One-third was randomly assigned as training samples and the other two-thirds as validating samples. For RF and SVM classifiers, optimal calibration models were defined by a 10 cross-fold validation sampling method. For the Random Forest classifier, the optimal number of trees to grow and number of variables randomly sampled at each split were set at 1000 and 4 respectively. For the Support Vector Machine classifier, optimal gamma and cost values were set at 0.5 and 128 respectively. Finally, a 3×3 median filter was applied to reduce salt-and-pepper effects. Once classified, habitat maps derived from each dataset were crossed with validation

samples ($n = 30$ by class \times 9 classes) in order to derive a confusion matrix, an accuracy index and a global Kappa index (Congalton et al., 1983).

To assess the interest of bi-seasonal images to map plant community combinations, we select the best supervised method and compared the classification accuracy using many combinations of Landsat images: one based on the summer image, one based on the winter image and one based on bi-seasonal image. Remote sensing analysis were performed with ENVI 5.2 (ITT) software. SVM and RF classifications were applied in e1071 (Dimitriadou et al., 2011), randomForest (Liaw and Wiener, 2002) and raster (Hijmans and van Etten, 2012) R-packages.

Results

Coastal marshes were found to cover 4630 km² and were correctly delineated based on topographical criteria. The Maximum Likelihood classification of the bi-seasonal images reliably discriminates the various habitat classes in coastal marshlands (Fig. 3). The classification accuracy ranges from 66.9 to 85.9 % for the Mahalanobis and Maximum Likelihood classifiers, respectively (Table 3). The bi-seasonal analysis has better results (85.9 % overall accuracy) than the mono-seasonal analysis (76.1 and 63.1 % overall accuracy for summer and winter images respectively), regardless of the class considered (Table 4): water, *Beto maritimae-Agroropyreto pungentis* geosigmetum, *Senecio aquatici-Oenantheo silaifoliae* geosigmetum, evergreen woods, deciduous woods, sand and vegetal dune areas are successfully discriminated, with low under- and over-detection error values (< 14 %). *Puccinellio maritimae-Arthrocnemeto fruticosi* geosigmetum, *Trifolio maritimae-Oenantheo silaifoliae* geosigmetum, reeds, impervious and salt pan areas are also well identified with under- and over-detection error values less than 25 %. Crops are moderately well classified (over-detection error value of 43.2 %) and are confused with reeds and impervious areas which have similar spectral signatures. In September, corn crops and reeds experience significant growth, reaching heights greater than 1.5 m. In December, reeds have a high dry matter density that could be confused with thatched corn and some agricultural lands with bare soil can be confused with impervious areas.

For all the marshlands studied, the variation in vegetation from the sea to the uplands is accurately recognized using the Landsat image classification. For example, *Beto maritimae-Agroropyreto pungentis* geosigmetum is widely spread in the Guérande marsh, Noirmoutier marsh and in the Aiguillon sur Mer bay; the *Puccinellio maritimae-Arthrocnemeto fruticosi* geosigmetum and salt pans are mapped with high proportions in the Guérande, Breton, Brouage and Seudre marshes; the *Trifolio maritimae-Oenantheo silaifoliae*

Fig. 3 Classification of the landscape unit for the Atlantic coastal marshlands derived from Landsat-8 images. Delineation of marshlands was based on the SRTM with a 90 m horizontal uncertainty

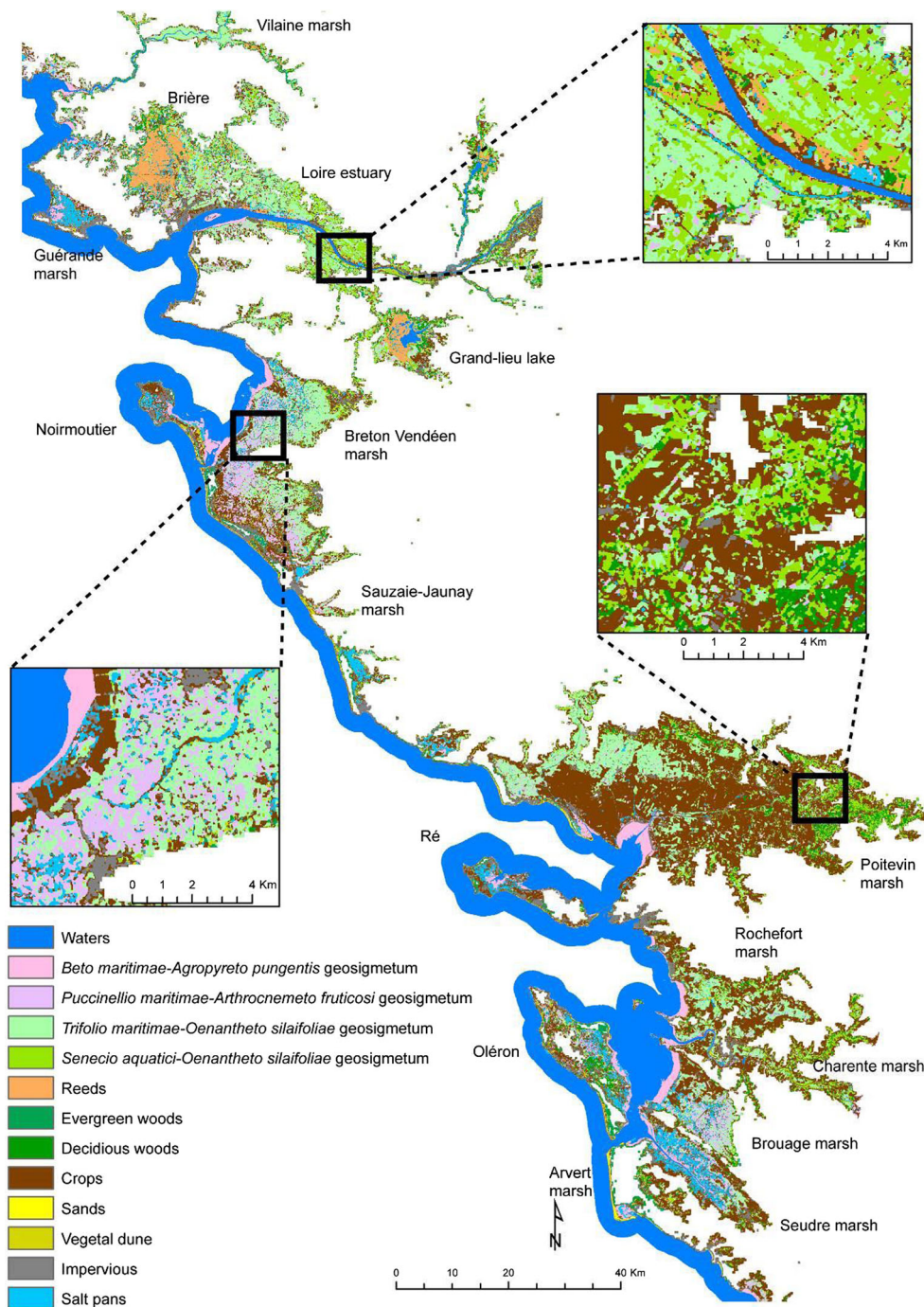


Table 3 Comparison of most frequently used classification algorithms for coastal habitat mapping derived from bi-seasonal Landsat 8 images

Classifier	Kappa index	Overall accuracy (%)
Mahalanobis	0.64	66.9
Minimal distance	0.66	68.8
Random Forest	0.78	80.0
Support Vector Machine	0.80	81.5
Maximum likelihood	0.85	85.9

geosigmetum class is widely distinguished in the Loire estuary, Breton marsh, Poitevin marsh and Rochefort marsh; and *Senecio aquatici-Oenantheto silaifoliae* geosigmetum habitats are present in the Loire estuary, on the continental edge of the marshes. Reeds are mainly developed in the Brière marsh and on the border of the Grand-Lieu Lake as well as, more locally, in the Breton and Rochefort marshes. Evergreen woods are identified on back dune whereas deciduous woods are classified on the lower parts of the marshes, near the foot slope. Crops are recognized and mapped on the polders in the

Table 4 Under- (A) and over-detection rates (B) expressed in percent per class for the vegetation classifications taken from mono-temporal and bi-seasonal Landsat-8 images, using the Maximum likelihood classifier

Satellite images	L8 03/09/2013		L8 08/12/2013		L8 03/09/2013 L8 08/12/2013	
	A	B	A	B	A	B
Water	13.3	00.0	20.0	31.4	10.0	00.0
<i>Beto maritimae-Agropyreto pungentis</i> geosigmetum	16.7	00.0	50.0	40.0	06.6	00.0
<i>Puccinellio maritimae-Arthrocnemeto fruticosi</i> geosigmetum	36.7	34.4	50.0	16.7	10.0	25.0
<i>Trifolio maritimae-Oenantheto silaifoliae</i> geosigmetum	30.0	34.4	90.0	57.1	03.3	19.4
<i>Senecio aquatici-Oenantheto silaifoliae</i> geosigmetum	30.0	00.0	03.3	71.6	13.3	13.3
Reeds	20.0	17.2	53.3	39.1	30.0	00.0
Evergreen woods	33.3	09.1	30.0	08.7	13.3	03.7
Deciduous woods	10.0	12.9	23.3	30.3	03.3	03.3
Crops	30.0	61.8	20.0	36.8	16.7	43.2
Sands	20.0	00.0	10.0	06.9	23.3	00.0
Vegetal dune	40.0	35.7	36.6	00.0	26.6	04.3
Impervious	23.3	08.0	33.3	16.7	16.7	24.2
Salt pans	06.7	34.8	60.0	14.3	10.0	15.6
Kappa index	0.74		0.60		0.85	
Global accuracy (%)	76.1		63.1		85.9	

Breton marsh and on the island of Noirmoutier as well as in Poitevin marsh.

A spatial analysis derived from the Landsat classification showed that the studied area comprises 854 km² of *Trifolio maritimae-Oenantheto silaifoliae* geosigmetum, 403 km² of *Puccinellio maritimae-Arthrocnemeto fruticosi* geosigmetum and 286 km² of *Beto maritimae-Agropyreto pungentis* geosigmetum (Table 5). Crops, including wheat, corn and sunflower represent more than 35 % of the total area of the marshlands: this reflects that a significant portion of the marshland natural habitat type is being lost to agriculture for the 1950's (Godet and Thomas, 2013), principally as a result of conversion to arable farmland (Duncan et al., 1999). For only two habitat classes (*Trifolio maritimae-Oenantheto silaifoliae* geosigmetum and crops), the average size of the patches is larger than 30.10⁻³ km². For the other classes, the size of the habitat patches ranges from 8.10⁻³ to 21.10⁻³ km², with high standard deviation values from one patch to the other that reveals a heterogeneous spatial structure of plant communities.

Discussion

Vegetation Classifications in Coastal Marshes Using Landsat Data

The goal of this work was to assess whether marshland plant community combinations may be efficiently mapped at the

1:50,000 scale, a suitable scale for management and monitoring, using free Landsat 8 OLI images. The challenge, which was to our knowledge addressed in this study for the first time, consists in using Landsat 8 OLI images with a 30 m pixel size to reliably map fine-grained vegetation but at regional scale. This was effectively achieved as we identified and located the geosigmetum, with 85 % accuracy over the 4630 km² marshland region.

This study proves that the challenge of mapping plant community combination is achievable, even with fine-grained spatially heterogeneous vegetation. The approach suggested here goes beyond the physiognomy-based approach to vegetation conducted on Landsat images by Baker et al., 2006; MacAlister and Mahaxay, 2009; Ottinger et al., 2013; Akumu et al., 2010; Cardoso et al., 2013; Sanchez-Hernandez et al., 2007, as it provided information regarding the probable plant communities and thereafter probable species composition. It also proved successful to detect a wide range of habitat types, even when combined in a fine-grained landscape, and including both inland and tidal marshes.

Some other studies had focused on only small tidal marsh sites with homogeneous dominant plant species for each Landsat pixel and therefore handled a simple vegetation structure. For example, Carreño et al., 2008 mapped salt marshes, salt steppes and reeds in a 5 km² area of wetland; similarly, Li et al., 2010; Zhang et al., 2011 discriminated only three habitat classes (*Suaeda salsa*, *Spartina anglica* and *Spartina alterniflora*) on a 100 km² salt marsh site. Recent work by Valentini et al. (2015) also aimed to map heterogeneous vegetation, approached by the dominant plant species, but the

Table 5 Total area, percentage of landscape, mean area and standard deviation of the patches for each class (water was excluded in the calculation). Delineation of marshlands was based on the SRTM with a 90 m horizontal uncertainty

Mapped classes	Total area km ²	Percentage	Mean area km ²	Standard deviation km ²
Crops	1 688	36.4	49.10 ⁻³	3.30
<i>Trifolio maritimae-Oenantheto silaifoliae</i> geosigmetum	854	18.4	37.10 ⁻³	0.72
<i>Puccinellio maritimae-Arthrocnemeto fruticosi</i> geosigmetum	403	8.7	19.10 ⁻³	0.23
Impervious	389	8.4	21.10 ⁻³	0.20
<i>Senecio aquatici-Oenantheto silaifoliae</i> geosigmetum	324	7.0	14.10 ⁻³	0.08
Salt pans	286	6.2	17.10 ⁻³	0.20
Deciduous woods	167	3.6	14.10 ⁻³	0.07
<i>Beto maritimae-Agropyreto pungentis</i> geosigmetum	161	3.5	41.10 ⁻³	0.70
Reeds	143	3.1	13.10 ⁻³	0.61
Evergreen woods	102	2.2	8.10 ⁻³	0.06
Vegetal dunes	93	2.0	4.10 ⁻³	0.01
Sands	24	0.5	11.10 ⁻³	0.10

classification accuracy remained moderate, with a 0.62 Kappa index value. In our study, we successfully mapped heterogeneous vegetation (Kappa index value 0.85) by considering plant communities' combinations or a geosigmetum approach. This map may be joined to a vegetation summary table which highlights the combinations of vegetal associations as the percentage occurrence of plant communities (Géhu, 2011). As a result, mapping vegetation using geosigmetum may be used for localizing habitats with specific interest: for example, the *Alopecuro-Juncetum gerardii*, a plant community of European interest (CORINE Biotope code 15.331) is likely to occur where the geosigmetum "*Trifolio maritimae-Oenantheto silaifoliae*" was identified on the basis of landsat images (Table 1). Predicting the "potential habitat" of a plant community of European interest may be extremely useful to locate detailed monitoring on the field or using very high spatial and spectral resolution sensors (Roelofsen et al., 2014).

The quality of the map that was produced may be first related to the 12-bit spectral depth of the Landsat 8 OLI sensor. A comparison between the 8-bit Landsat-7 ETM and the 12-bit Landsat-8 OLI images showed that a high spectral depth improves the class separability (Jia et al., 2014). In addition, the use of bi-seasonal image increases the accuracy of vegetation mapping (the Kappa index increased from 0.74 to 0.85) as also found by Rapinel et al. (2015). September and December Landsat 8 images can thus be used complementary for vegetation mapping. In September, environmental contrasts between drylands and wetlands were enhanced and accordingly their spectral separability; same was found for the separability between highly drained sub-brackish habitats and wet fresh habitats. The image acquired in December distinguished well the reeds beds, thanks to their high standing dry matter, and discriminate efficiently evergreen woods from deciduous woods and crops from grasslands.

Despite the high overall accuracy of the classification, some confusion was observed between crops and reeds or between *Puccinellio maritimae-Arthrocnemeto fruticosi* geosigmetum and *Trifolio maritimae-Oenantheto silaifoliae* geosigmetum. Additional images taken at different seasons may probably improve the quality of classification (Schuster et al., 2015). This was not possible in our study as additional cloud-free images covering the regional study area were unavailable in 2013.

The best classification accuracy was obtained with the maximum likelihood classifier while random forest and support vector machine classifiers produced close accuracies. Currently, a wide range of classifiers have been used for coastal vegetation mapping derived from Landsat images: maximum likelihood classifier (Isacch et al., 2006; Carreño et al., 2008; Zhang et al., 2011; Akumu et al., 2010); support vector machine classifier (Sanchez-Hernandez et al. 2007); spectral angle mapper classifier (Cardoso et al. 2013); decision tree classifier (Ottinger et al. 2013) or the minimum distance classifier (Li et al. 2010). Accordingly, there is no clear consensus on the most suitable classifier for vegetation mapping since the efficiency of each classifier depends on: (i) the type and number of training samples available, (ii) the class similarity in the typology, (iii) the characteristics of the images used.

A limitation of the geosigmetum approach concerns the Modifiable Areal Unit Problem and its implications for landscape ecology (Jelinski and Wu, 1996). As already highlighted by Schmidlein (2003), the spatial aggregation of vegetation patches and pixel size has an impact on the resulting patterns and vegetation patterns with a very fine-grained spatial structure (< 50 m) may be underestimated using the Landsat classification. As a result, the Landsat classification should be considered at the 1:50,000 scale, and that misinterpretation might arise if used at a finer scale.

Benefits of Regional-Scale Marsh Mapping for Conservation

The combinations of plant communities that were mapped in this study covered approximately 30 % of the French Atlantic coastline. The subsequent contrasts in the plant community combination were remarkably detected by the multispectral Landsat OLI data despite the poor contrasts in their physiognomy. This detection may provide important information of the environmental conditions prevailing in the different marshes. Indeed, *Puccinellio maritimae-Arthrocnemeto fruticosi* geosigmetum can be discriminated from *Trifolium maritimae-Oenantheto silaifoliae* geosigmetum in the Breton-Vendéen and Seudre marshes. This geosigmetum can be considered as patrimonial landscape since their plant assemblage is remarkable as it results from salt water irrigation which remains nowadays in very few Atlantic marshes. Conversely, in the Poitevin and Rochefort marshes, only *Trifolium maritimae-Oenantheto silaifoliae* geosigmetum and *Senecio aquatici-Oenantheto silaifoliae* geosigmetum were distinguished from the Landsat image classification, as only freshwater is circulating in the ditches (Verger, 2005).

The approach we used, based on Landsat images, thus opens a new avenue for plant community monitoring. There is indeed still a clear need for vegetation mapping and survey methods, even in the widely described French Atlantic coastal habitats as only few local vegetation maps are available from very high spatial remote sensing images (Godet and Thomas 2013; Rapinel et al., 2014; Sawtschuk and Bioret 2012; Murgues et al., 2014).

When focusing on the quality of the map produced in this study, a key point is its close concordance with vegetation maps derived from very high spatial remote sensing images: (i) the *Beto maritimae-Agropyreto pungentis* geosigmetum and crop areas are located in a similar location and with similar extents to salt marshes and crops mapped in 2008 from aerial photograph analysis on the Poitevin marsh (Godet and Thomas 2013); (ii) the *Trifolium maritimae-Oenantheto silaifoliae* geosigmetum and dunes are mapped with a similar extent to “hygrophilous grasslands” and “grasslands on fixed sands” classified from Worldview-2 imagery on the Sauzaie marsh (Rapinel et al., 2014); (iii) Sawtschuk and Bioret (2012) used LiDAR data and field observations on a 4 km² Loire estuary site to map salt tolerant vegetation, such as *Bolboschoenus maritimus* which dominated vegetation in *Puccinellia maritima* meadows and *Phragmites australis*: our results are consistent with their survey with a vegetation map based on Landsat-8 OLI which clearly identified and located reeds and *Puccinellio maritimae-Arthrocnemeto fruticosi* geosigmetum, (iv) where the Pléiades image detected *Phragmites australis*, *Phalaris arundinacea* and *Cladium mariscus* on the Brière site (Murgues et al., 2014), reed habitats were mapped using Landsat-8.

Satellite based vegetation map can constitute an efficient tool for environmental management at the regional scale: with their large footprint width (185 km), covering the whole watershed, Landsat 8 OLI can be used as a support for environmental policies related to biodiversity, conservation and ecosystem services. This may be particularly useful within the framework of the European Union habitat Directive 92/43/EEC and the French strategy for biodiversity (2011–2020) which require ad hoc monitoring of the natural and semi-natural habitats. The method developed in this study could be easily repeatable in time and space for understanding impacts of ecological interactions, climate change and anthropic pressures on ecological changes (Kennedy et al., 2014). The recent open-access of Landsat images and long term data continuity should promote their use by managers and biologists where there is a strong need for spatialized data (Turner et al., 2015). The regional geosigmetum map derived from Landsat-8 may indeed complement pan-European habitat maps which only have a coarse resolution based on a 10 × 10 km grid (Schmeller et al., 2014). At the global scale, our approach highlights the interest of Landsat 8 OLI for completing and downscaling the map of the global relative abundance of salt marsh habitats provided by the World Conservation Monitoring Centre (Hoekstra et al., 2010) and also describes global change adaptation of marsh plant communities (Saintilan et al., 2014).

Considering that plant communities are indicators of ecological factors (Grime, 2006), mapping the plant community's combination constitutes a basis for a spatialized assessment of wetland functions and ecological services at regional scale, as conducted for example on Amazonian pioneer fronts by Grimaldi et al., 2014.

Acknowledgments This research was funded by the CarHab project (French Ministry of Ecology and Sustainable Development). The authors thank Olivier Gore for his help in the field; Nicolas Rossignol, Renan Leroux and Alban Thomas for their help in data analysis; the GIP Loire Estuaire, DREAL Pays de la Loire, DREAL Poitou Charentes, and the Parc Naturel Régional du Marais Poitevin for providing the field-based vegetation maps.

References

- Akumu CE, Pathirana S, Baban S, Bucher D (2010) Monitoring coastal wetland communities in north-eastern NSW using ASTER and Landsat satellite data. *Wetl Ecol Manag* 18:357–365
- Amiaud B, Bouzillé JB, Tournade F, Bonis A (1998) Spatial patterns of soil salinities in old embanked marshlands in western France. *Wetlands* 18:482–494
- Baker C, Lawrence R, Montagne C, Patten D (2006) Mapping wetlands and riparian areas using Landsat etm1 imagery and decision-tree-based models. *Wetlands* 26:465–474
- Barillé L, Robin M, Harin N, Bargain A, Launeau P (2010) Increase in seagrass distribution at bourgneuf bay (France) detected by spatial remote sensing. *Aquat Bot* 92:185–194

- Berberoglu S, Yilmaz KT, Özkan C (2004) Mapping and monitoring of coastal wetlands of çukurova delta in the eastern Mediterranean region. *Biodivers Conserv* 13:615–633
- Biondi E, Casavecchia S, Pesaresi S (2011) Spontaneous renaturalization processes of the vegetation in the abandoned fields (central Italy). *Ann di Bot* 6:65–94
- Bouzillé JB, Kernéis E, Bonis A, Touzard B (2001) Vegetation and ecological gradients in abandoned salt pans in western France. *J Veg Sci* 12:269–278
- Breiman L (2001) Random forests. *Mach Learn* 45:5–32
- Cardoso GF, Jr CS, PWM S-F (2013) Using spectral analysis of landsat-5 TM images to map coastal wetlands in the amazon river mouth, Brazil. *Wetl Ecol Manag* 22:79–92
- Carreño MF, Esteve MA, Martínez J, et al (2008) Habitat changes in coastal wetlands associated to hydrological changes in the watershed. *Estuar Coast Shelf Sci* 77:475–483
- Chauveau E, Chadenas C, Comentale B, Pottier P, Blanckœil A, Feuillet T, Mercier D, Pourinet L, Rollo N, Tillier I, Trouillet B (2011) Xynthia: lessons of a disaster. *Cybergeo: Eur J Geogr*. doi:10.4000/cybergeo.23763
- Cingolani AM, Renison D, Zak MR, Cabido MR (2004) Mapping vegetation in a heterogeneous mountain rangeland using Landsat data: an alternative method to define and classify land-cover units. *Remote Sens Environ* 92:84–97
- Congalton RG, Oderwald RG, Mead RA (1983) Assessing Landsat Classification accuracy using discrete multivariate analysis statistical techniques. *Photogramm Eng Remote Sens* 49:1671–1678
- Decocq G (2002) Patterns of plant species and community diversity at different organization levels in a forested riparian landscape. *J Veg Sci* 13:91–106
- Dimitriadou E, Hornik K, Leisch F, et al (2011) e1071: misc functions of the department of statistics (e1071), TU Wien. R Package version 1.5–27.
- Dumont B, Rossignol N, Loucougaray G, Carrère P, Chadoeuf J, Fleurance G, Bonis A, Farruggia A, Gaucherand S, Ginane C, Louault F, Marion B, Mesléard F, Yaverkovski N (2012) When does grazing generate stable vegetation patterns in temperate Pastures? *Agric Ecosyst Environ* 153:50–56
- Duncan P, Hewison AJM, Houte S, Rosoux R, Tournebize T, Dubs F, Burel F, Bretagnolle V (1999) Long-term changes in agricultural practices and wildfowling in an internationally important wetland, and their effects on the guild of wintering ducks. *J Appl Ecol* 36:11–23
- Géhu J-M (2011) On the opportunity to celebrate the centenary of modern phytosociology in 2010. *Plant Biosyst* 145:4–8
- Géhu JM, Bouzille JB, Bioret F, Godeau M, Botineau M, Clément B, Touffet J, Lahondere C (1991) Approche paysagere symphytosociologique des Marais littoraux du centre-Ouest de la France. *Colloques Phytosociologique Phytosociologie et Paysages* 17:109–127
- Godet L, Thomas A (2013) Three centuries of land cover changes in the largest French Atlantic wetland provide new insights for wetland conservation. *Appl Geogr* 42:133–139
- Grimaldi M, Oszward J, Dolédec S, et al (2014) Ecosystem services of regulation and support in Amazonian pioneer fronts: searching for landscape drivers. *Landsc Ecol* 29:311–328
- Grime JP (2006) Plant strategies, vegetation processes, and ecosystem properties. John Wiley & Sons, Chichester
- Hijmans RJ, van Etten J (2012) Raster: geographic analysis and modeling with raster data. R Package Version 2.0–12
- Hoekstra JM, Molnar JL, Jennings M, et al (2010) The atlas of global conservation: changes, challenges and opportunities to make a difference. University of California Press Berkeley, CA
- Isacch JP, Costa CSB, Rodríguez-Gallego L, Conde D, Escapa M, Gagliardini DA, Iribarne OO (2006) Distribution of saltmarsh plant communities associated with environmental factors along a latitudinal gradient on the south-west Atlantic coast. *J Biogeogr* 33:888–900
- Jarvis A, Reuter H, Nelson A, Guevara E (2008) Hole-filled SRTM for the globe Version 4. Available from the CGIAR-CSI SRTM 90 m database. <http://srtm.csi.cgiar.org>
- Jelinski DE, Wu J (1996) The modifiable areal unit problem and implications for landscape ecology. *Landsc Ecol* 11:129–140
- Jia K, Wei X, Gu X, Yao Y, Xie X, Li B (2014) Land cover classification using Landsat 8 Operational Land Imager data in Beijing, China. *Geocarto International* 1–11
- Kennedy RE, Andréfouët S, Cohen WB, et al (2014) Bringing an ecological view of change to Landsat-based remote sensing. *Front Ecol Environ* 12:339–346
- Kirwan ML, Guntenspergen GR, D’Alpaos A, Morris JT, Mudd SM, Temmerman S (2010) Limits on the adaptability of coastal marshes to rising sea level. *Geophys Res Lett* 37:L23401
- Lang S, Mairota P, Pernkopf L, Schioppa EP (2015) Earth observation for habitat mapping and biodiversity monitoring. *Int J Appl Earth Obs Geoinf* 37:1–6
- Lee TM, Yeh HC (2009) Applying remote sensing techniques to monitor shifting wetland vegetation: a case study of Danshui river estuary mangrove communities, Taiwan. *Ecol Eng* 35: 487–496
- Leguédou S, Party JP, Dupouey JL, Gauquelin T, Gégout JC, Lecareux C, Badeau V, Probst A (2011) The vegetation map of the CNRS going numerical: the geographical database of the vegetation of France. *Cybergeo: Eur J Geogr*. doi:10.4000/cybergeo.24688
- Li J, Gao S, Wang Y (2010) Invading cord grass vegetation changes analyzed from Landsat-TM imageries: a case study from the wanggang area, Jiangsu coast, eastern China. *Acta Oceanol Sin* 29:26–37
- Liaw A, Wiener M (2002) Classification and regression by randomForest. *R News* 2:18–22
- MacAlister C, Mahaxay M (2009) Mapping wetlands in the lower Mekong basin for wetland resource and conservation management using Landsat ETM images and field survey data. *J Environ Manag* 90:2130–2137
- Marion B, Bonis A, Bouzillé J-B (2010) How much does grazing-induced heterogeneity impact plant diversity in wet grasslands? *Ecoscience* 17:229–239
- Mitsch WJ, Gosselink JG (2007) *Wetlands*. John Wiley and Sons, Inc., Hoboken
- Mountrakis G, Im J, Ogole C (2011) Support vector machines in remote sensing: a review. *ISPRS J Photogramm Remote Sens* 66:247–259
- Murgues M, Marquet M, Debaine F (2014) Cartographie des formations végétales des zones humides du parc naturel régional de brière par analyse d’image orientée-objet. *Les Cahiers Nantais* 5–16(in french)
- Ottinger M, Kuenzer C, Liu G, et al (2013) Monitoring land cover dynamics in the yellow river delta from 1995 to 2010 based on Landsat 5 TM. *Appl Geogr* 44:53–68
- Ozenda P, Lucas MJ (1987) Esquisse d’une carte de la végétation potentielle de la France à 1/1 500 000. *Documents Cartographie écologique* 30:49–80
- Rapinel S, Clément B, Magnanon S, Sellin V, Hubert-Moy L (2014) Identification and mapping of natural vegetation on a coastal site using a worldview-2 satellite image. *J Environ Manag* 144:236–246
- Rapinel S, Hubert-Moy L, Clément B (2015) Combined use of LiDAR data and multispectral earth observation imagery for wetland habitat mapping. *Int J Appl Earth Obs Geoinf* 37: 56–64
- Richards JA (1999) *Remote sensing digital image analysis: an introduction*. Springer-Verlag, New York

- Rivas-Martinez S (2005) Notions on dynamic-catenal phytosociology as a basis of landscape science. *Plant Biosyst* 139:135–144
- Roelofs HD, Kooistra L, van Bodegom PM, Verrelst J, Krol J, Witte JPM (2014) Mapping a priori defined plant associations using remotely sensed vegetation characteristics. *Remote Sens Environ* 140: 639–651
- Saintilan N, Wilson NC, Rogers K, et al (2014) Mangrove expansion and salt marsh decline at mangrove poleward limits. *Glob Chang Biol* 20:147–157
- Sanchez-Hernandez C, Boyd DS, Foody GM (2007) Mapping specific habitats from remotely sensed imagery: support vector machine and support vector data description based classification of coastal saltmarsh habitats. *Ecol Inf* 2:83–88
- Sawtschuk J, Bioret F (2012) Diachronic analysis of vegetation spatial dynamic in Loire estuary. *Photo-Interpretation* 48:15–28
- Schmeller DS, Evans D, Lin Y-P, Henle K (2014) The national responsibility approach to setting conservation priorities—recommendations for its use. *J Nat Conserv* 22:349–357
- Schmidtlein S (2003) Raster-based detection of vegetation patterns at landscape scale levels. *Phytocoenologia* 33:603–621
- Schuster C, Schmidt T, Conrad C, et al (2015) Grassland habitat mapping by intra-annual time series analysis – comparison of RapidEye and TerraSAR-X satellite data. *Int J Appl Earth Obs Geoinf* 34:25–34
- Turner W, Rondinini C, Pettorelli N, et al (2015) Free and open-access satellite data are key to biodiversity conservation. *Biol Conserv* 182: 173–176
- Valentini E, Taramelli A, Filippini F, Giulio S (2015) An effective procedure for EUNIS and Natura 2000 habitat type mapping in estuarine ecosystems integrating ecological knowledge and remote sensing analysis. *Ocean Coast Management* 108:52–64
- Van der Maarel E (2005) *Vegetatio ecology – an overview*. In : *Vegetation ecology*. Edit eddy van der maarel. 1–51. Blackwell Publishing, Malden.
- Vanden Borre J, Paelinckx D, Mûcher CA, Kooistra L, Haest B, De Blust G, Schmidt AM (2011) Integrating remote sensing in Natura 2000 habitat monitoring: prospects on the way forward. *J Nat Conserv* 19: 116–125
- Verger F (2005) *Marais et estuaires du littoral français*. Belin, Paris
- Xie Y, Sha Z, Yu M (2008) Remote sensing imagery in vegetation mapping: a review. *J Plant Ecol* 1:9–23
- Zak MR, Cabido M (2002) Spatial patterns of the Chaco vegetation of central Argentina: integration of remote sensing and phytosociology. *Appl Veg Sci* 5:213–226
- Zhang Y, Lu D, Yang B, et al (2011) Coastal wetland vegetation classification with a Landsat thematic mapper image. *Int J Remote Sens* 32:545–561